Supplementary Data

Roblek et al.

CCL2 is a vascular permeability factor inducing CCR2-dependent endothelial retraction during lung metastasis

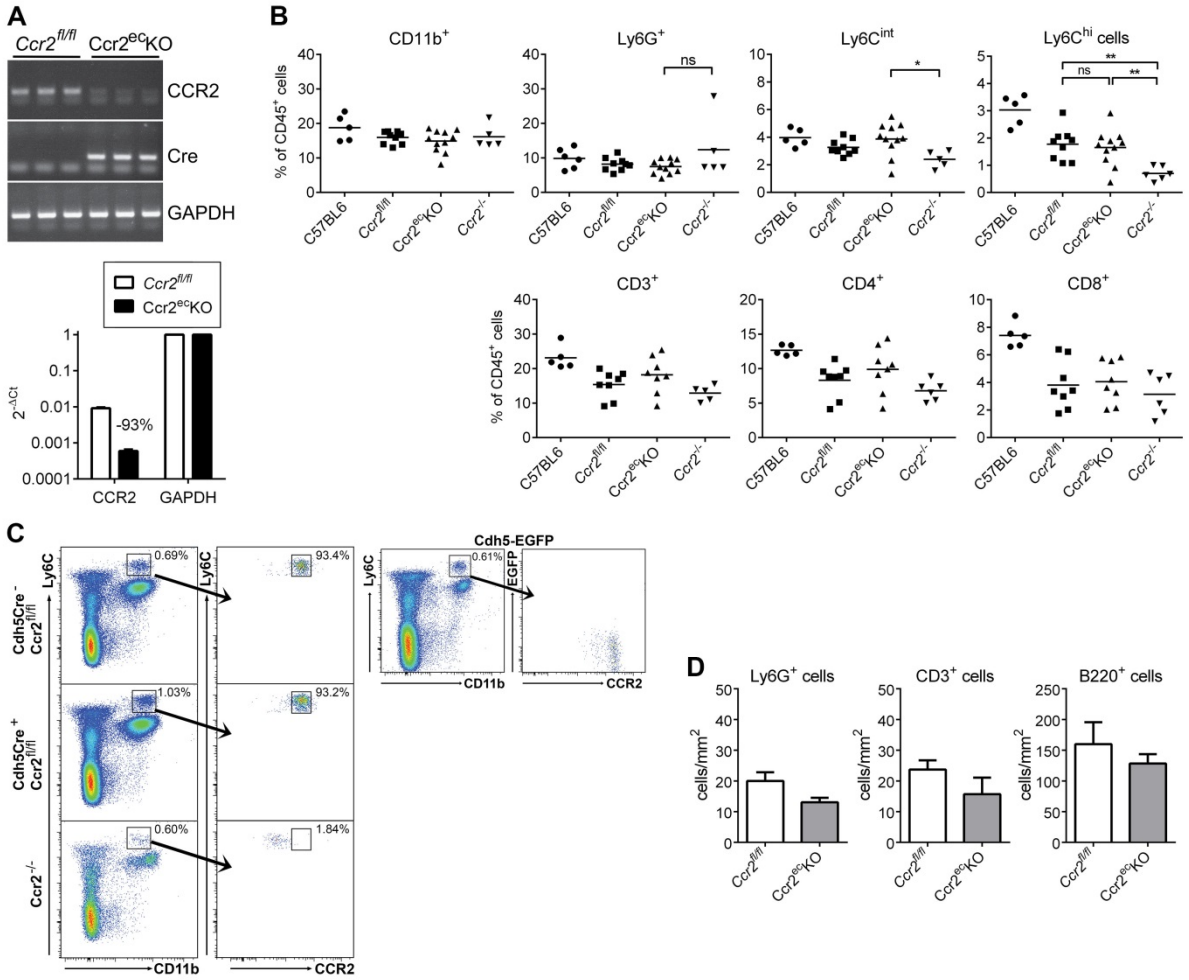

Supplementary Figure 1. Characterization of Ccr2^{ec}KO mice and analysis of primary tumors. A) Agarose gel electrophoresis of CCR2, Cre and GAPDH amplified from sorted pulmonary endothelial cells from *Ccr2$^{fl/fl}$* and Ccr2^{ec}KO littermates (top). Expression levels of sorted pulmonary endothelial cells from *Ccr2$^{fl/fl}$* and Ccr2^{ec}KO littermates by qPCR (bottom). Data are represented as relative expression levels ($2^{-\Delta ct}$) normalized to GAPDH. (*Ccr2$^{fl/fl}$* n=5; Ccr2^{ec}KO n=9). **B)** Flow cytometry analysis of relative amounts of myeloid cells (CD45$^+$CD11b$^+$), neutrophils (CD45$^+$CD11b$^+$Ly6G$^+$), Ly6C^{int} monocytes (CD45$^+$CD11b$^+$Ly6G$^-$Ly6C^{int}), inflammatory monocytes (CD45$^+$CD11b$^+$Ly6G$^-$Ly6C^{hi}), T cells (CD45$^+$CD3$^+$), CD4$^+$ T cells (CD45$^+$CD3$^+$CD4$^+$) and CD8$^+$ T cells (CD45$^+$CD3$^+$CD8$^+$) in peripheral blood of C57BL6, *Ccr2$^{fl/fl}$*, Ccr2^{ec}KO, and *Ccr2$^{-/-}$* mice. Statistical significance was assessed using unpaired t-test; **; p<0.01; *; p<0.05; ns = not significant. **C)** Flow cytometry analysis of CCR2 expression on circulating cells (CD11b$^+$Ly6C^{hi}) from Ccr2^{ec}KO, *Ccr2$^{fl/fl}$* and *Ccr2$^{-/-}$* mice. Analysis of the CCR2 expression on VE-cadherin-positive cells using a reporter mouse (Cdh5-GFP), expressing GFP under the VE-cadherin promoter (right panel). **D)** Histological analysis of primary tumors using Ly6G, CD3 and B220 antibodies.

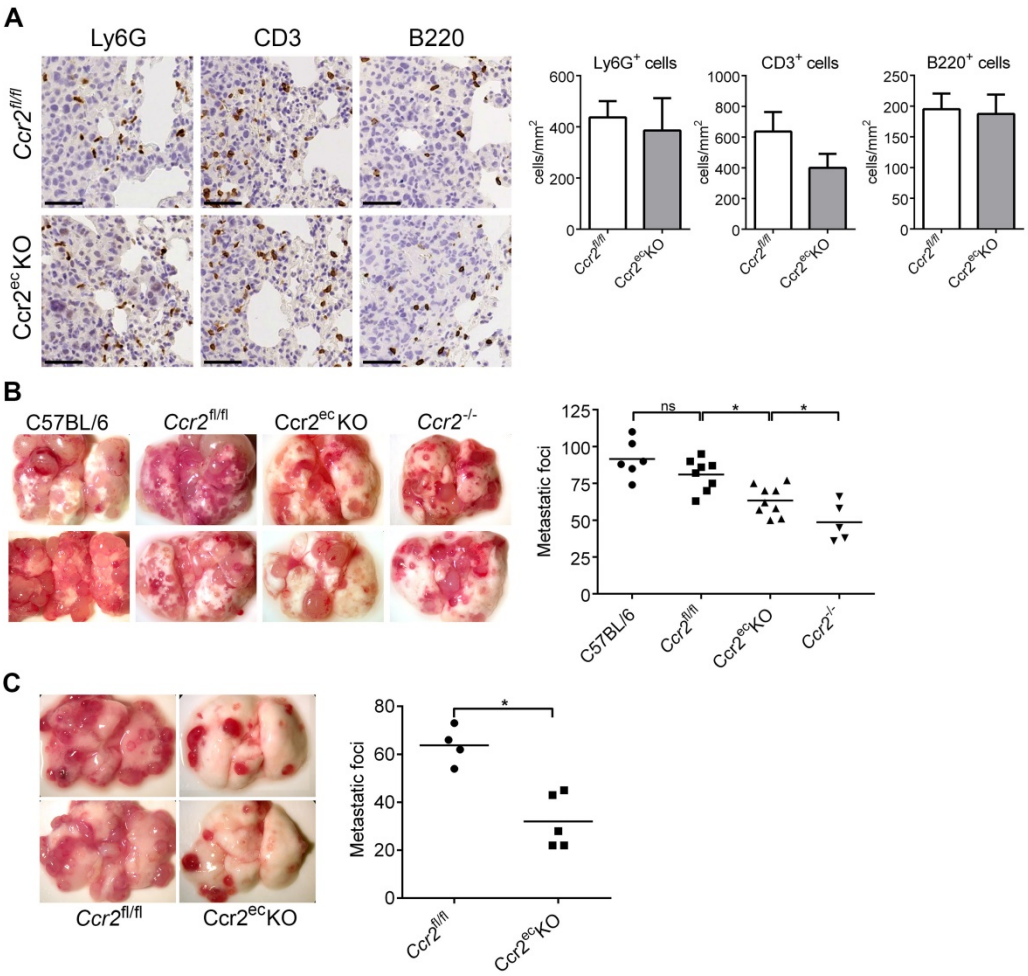

Supplementary Figure 2 Endothelial CCR2 is required for generation of spontaneous and experimental lung metastasis. A) Representative images of spontaneous lung metastasis stained with Ly6G, CD3, and B220 Abs, respectively were quantified. **B)** Experimental lung metastasis of i.v. injected MC-38GFP cells in C57BL/6, *Ccr2*$^{fl/fl}$, Ccr2^{ec}KO, and *Ccr2*$^{-/-}$ mice after 28 days. Representative lung images are shown in the left panel. **C)** Experimental metastasis in *Ccr2*$^{fl/fl}$ and Ccr2^{ec}KO mice 15 days after i.v. injection of LLC1.1 cells with corresponding representative lung images. *; p<0.05; **; p<0.01; ns = not significant.

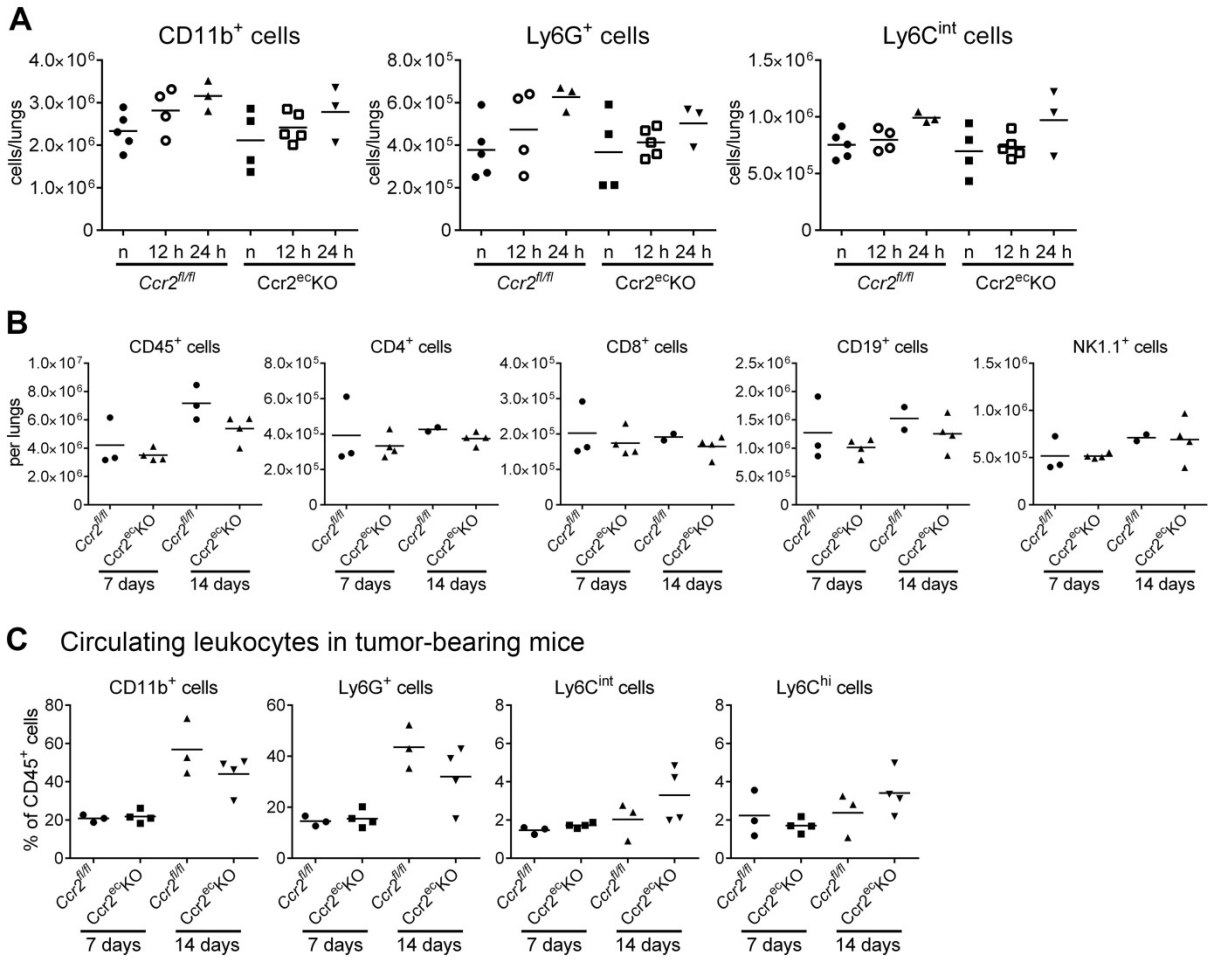

Supplementary Figure 3. Formation of the metastasis niche in the lungs is unaffected in Ccr2^{ec}KO mice. A) Flow cytometry analysis of myeloid cells (CD45$^+$CD11b$^+$), granulocytes (CD45$^+$CD11b$^+$Ly6G$^+$), and Ly6C^{int} monocytes (CD45$^+$CD11b$^+$Ly6G$^-$Ly6C^{int}) recruited to lungs 12 h and 24 h p.i. in *Ccr2$^{fl/fl}$* and Ccr2^{ec}KO mice. n = untreated naive mice. **B)** Flow cytometry analysis of CD45$^+$ cells, T cells (CD45$^+$CD11b$^-$CD19$^-$CD3$^+$), B cells (CD45$^+$CD11b$^-$CD19$^+$), NK cells (CD45$^+$CD11b$^-$CD19$^-$CD3$^-$NK1.1$^+$), CD4$^+$ T cells (CD45$^+$CD11b$^-$CD19$^-$CD3$^+$CD4$^+$), and CD8$^+$ T (CD45$^+$CD11b$^-$CD19$^-$CD3$^+$CD8$^+$) cells recruited to lungs of mice s.c.-injected with LLC cells after 7 and 14 days. **C)** Flow cytometry analysis of myeloid cells (CD45$^+$CD11b$^+$), granulocytes (CD45$^+$CD11b$^+$Ly6G$^+$), Ly6C^{int} monocytes (CD45$^+$CD11b$^+$LyG$^-$Ly6C^{int}), and inflammatory monocytes (CD45$^+$CD11b$^+$Ly6C^{hi}Ly6G$^-$) in the circulation of mice s.c.-injected with LLC cells after 7 and 14 days.

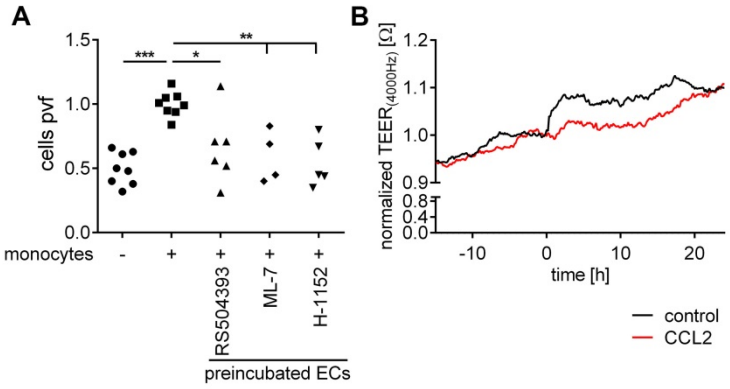

Supplementary Figure 4. Inhibition of CCL2-induced endothelial retraction attenuates tumor cell migration. A) Trans-endothelial migration of 4T1 murine breast cancer cells in the presence (+) or the absence (-) of $CD115^+$ monocytes after 16 hours. Endothelial cells were pre-treated with RS-504393 (50 µM), ML-7 (1 µM), and H-1152 (5 µM) for two hours and washed out of the inhibitor prior to adding of 4T1 cells with/without monocytes. The number of transmigrated cells was counted per view field (pvf) and is normalized to the control (+ monocytes). Statistical significance was assessed using unpaired t-test; *; $p<0.05$; **; $p<0.01$; ***; $p<0.001$. **B)** TEER values for rhCCL2-treated and control samples were normalized to 1 at the start of stimulation (0 h). TEER measurement profile over time (lower panel) (alternative presentation of data shown in Figure 4D).

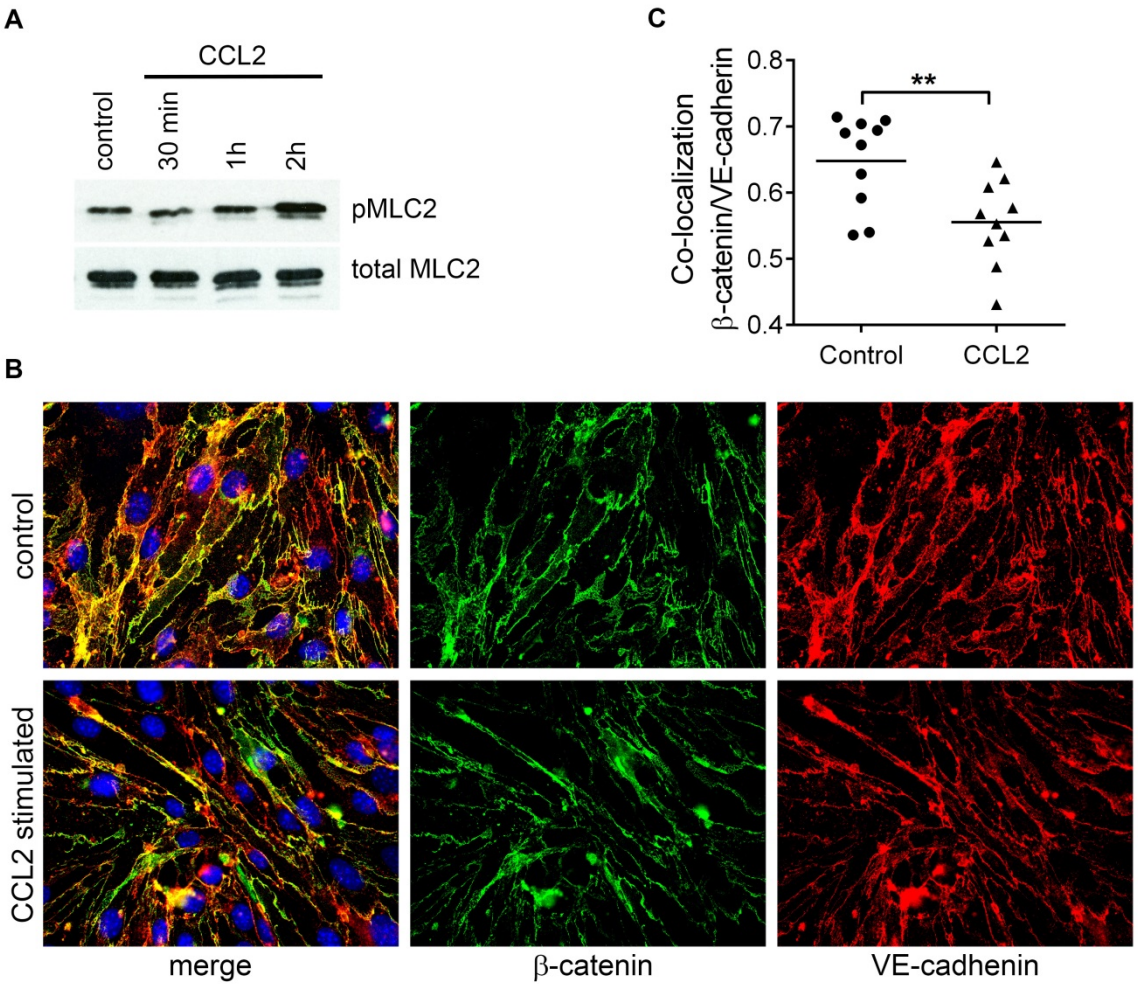

Supplementary Figure 5. CCL2 stimulation of endothelial cells induces phosphorylation of myosin-light chain 2 and dissociation of VE-cadherin/b-catenin complexes. A) Immune-detection of phosphorylated MLC2 (pMLC2) in the lysates of bEnd.3 endothelial cells after pre-activation with IL1-β and stimulation with CCL2 (100 ng/ml) for indicated time points. Total MLC2 detection served as control. Per lane 20 µg of protein lysate were loaded. **B)** Co-localization analysis of β-catenin with VE-cadherin expression in bEnd.3 cells. Endothelial cell line bEnd.3 was stimulated with 40ng/ml of IL1-β for 2h, washed and activated with 100 ng/ml of CCL2 for 1h. Cells were fixed with ice-cold methanol, permeabilized with Saponin 0.1%, blocked with 1% BSA and stained sequentially with rabbit-anti-mouse β-catenin (D10A8, Cell Signaling) and rat-anti-mouse VE-cadherin (Cl. 11D4.1, BD) with respective secondary antibodies. **C)** Co-localization of β-catenin and VE-cadherin was quantified using Fiji software (Pearson's R value) analyzing 10 different view-fields, **; $p < 0.01$.

Table 1. Primer used in this work.

primer	5'-3'
Cre_fw	TGG CAG AAC GAA AAC GCT GG
Cre_rev	TCT GAC CCG GCA AAA CAG GT
CCR2_fw	ATC CAC GGC ATA CTA TCA ACA TC
CCR2_rev	CAA GGC TCA CCA TCA TCG TAG
E-Sel_fw	CGC CAG AAC AAC AAT TCC AC
E-Sel_rev	ACT GGA GGC ATT GTA GTA CC
VCAM-1_fw	GCG GTC TTG GGA GCC TCA AC
VCAM-1_rev	GTG ACT CGC AGC CCG TAG TG
SAA1+2_fw	TCG GGG GAA CTA TGA TGC TGC
SAA1+2_rev	CAC TGC GGC CAT GTC TGT TG
SAA3_fw	TGC ATC TTG ATC CTG GGA GTT GAC
SAA3_rev	CAT AGT TCC CCC GAG CAT GGA AG
S100A4_fw	TCA GGC AAA GAG GGT GAC AAG TTC
S100A4_rev	ATT GTC CCT GTT GCT GTC CAA GT
S100A8_fw	TCA CCA TGC CCT CTA CAA GAA TGA C
S100A8_rev	TGC CAC ACC CAC TTT TAT CAC CA
S100A9_fw	CAC TGC TCT TAC CAA CAT CTG TGA C
S100A9_rev	GGG TGT CAG GGT GTC CTT CC
GAPDH_fw	CCC AGC AAG GAC ACT GAG CAA
GAPDH_rev	GTG GGT GCA GCG AAC TTT ATT GAT G